

# VO<sub>2</sub>-based Multiple State Micro-Mechanical Memory

By

Rafmag Cabrera Pizarro

A thesis submitted in partial fulfillment of the requirements for the degree of

MASTER OF SCIENCE

in

ELECTRICAL ENGINEERING

UNIVERSITY OF PUERTO RICO

MAYAGÜEZ CAMPUS

2011

Approved by:

\_\_\_\_\_  
Nelson Sepulveda-Alancastro, PhD  
President, Graduate Committee

\_\_\_\_\_  
Date

\_\_\_\_\_  
Félix E. Fernández, PhD  
Member, Graduate Committee

\_\_\_\_\_  
Date

\_\_\_\_\_  
Manuel Toledo-Quiñones, PhD  
Member, Graduate Committee

\_\_\_\_\_  
Date

\_\_\_\_\_  
Lev Steinberg, PhD  
Representative of Graduate Studies

\_\_\_\_\_  
Date

\_\_\_\_\_  
Erick Aponte, PhD  
Chairperson of the Department

\_\_\_\_\_  
Date

## Abstract

A VO<sub>2</sub>-coated silicon micromechanical cantilever capable of achieving multiple positional states is presented. The demonstrated mechanical memory uses the bimorph cantilever tip displacement as the programming parameter, and light pulses from a laser diode as the actuation mechanism. The large contraction of the VO<sub>2</sub> thin film across its insulator-to-metal-transition (IMT) caused the bending of the bimorph cantilever structure. Absolute displacements up to 21 μm were achieved in steps of different magnitudes when laser pulses of the same amplitude are used. The magnitude of the displacement steps were normalized to similar values along the excursion through the IMT by changing the magnitude of the laser pulses, demonstrating that the magnitude of the displacement steps can be controlled. The cantilever structure consisted of a silicon micrometer-sized cantilever (350 μm long, 35 μm wide, 1 μm thick) coated with a 300 nm VO<sub>2</sub> thin film deposited by pulsed-laser deposition (PLD).

## Resumen

En este trabajo se presenta una micro-viga voladiza con una capa delgada de dióxido de vanadio, la cual es capaz de alcanzar múltiples estados estables de deflexión. Esta memoria mecánica utiliza la deflexión de la punta de la viga como el parámetro programable y utiliza pulsos de luz de un diodo de laser como el mecanismo de actuación. La contracción masiva de la capa delgada de VO<sub>2</sub> a través de su transición aislante-metálica (IMT por sus siglas en ingles), causa la deflexión de la estructura. Una deflexión absoluta de hasta 21 μm se obtuvo en escalones de diferentes magnitudes utilizando pulsos de luz con un incremento de intensidad constante. La magnitud de los escalones se logró normalizar a través del IMT al cambiar la magnitud de los pulsos de luz, demostrando que la magnitud del desplazamiento se puede controlar. La estructura consistía en una viga voladiza de silicio de 350 μm de largo, 35 μm de ancho y 1 μm de espesor; con una capa delgada de 300 nm de VO<sub>2</sub> depositada por láser pulsado (PLD por sus siglas en inglés).

To my Family...

## Acknowledgments

This thesis would not have been possible if it wasn't for the immense help I received from my advisor Dr. Nelson Sepulveda. I owe him my deepest gratitude for his support throughout my entire academic career. I learned everything I know about research from him. His unfailing encouragement has guided me through the hurdles of grad school, to a promising future. For that, I am forever thankful. I am also very grateful for the guidance given to me by Dr. Felix Fernandez. His incredible wisdom and experience has been proven invaluable in our work. I also want to thank my family for their unending support and patience throughout my entire life.

This material is based in part upon work supported by the National Science Foundation under Grant No. ECCS-0954406 (CAREER Program).

# Table of Contents

<b>Abstract.....</b>	<b>i</b>
<b>Resumen.....</b>	<b>ii</b>
<b>Acknowledgments .....</b>	<b>iv</b>
<b>Table of Contents .....</b>	<b>v</b>
<b>Table of Figures.....</b>	<b>vi</b>
<b>1 Introduction .....</b>	<b>1</b>
1.1 Motivation .....	1
1.2 Literature Review .....	3
1.3 Summary of the Following Chapters .....	4
<b>2 Theoretical Background.....</b>	<b>5</b>
2.1 “Memory” Concepts .....	5
2.2 A Simple Electronic Memory Cell.....	6
2.3 The Use of VO <sub>2</sub> in Memory Devices .....	7
2.4 Possible VO <sub>2</sub> Based Electro-Mechanical Memory .....	10
<b>3 Materials and Methods .....</b>	<b>12</b>
3.1 Silicon Micro-Cantilevers and VO <sub>2</sub> Deposition .....	12
3.2 Measurement System and Procedure .....	14
3.2.1 Measurement System .....	14
3.2.2 Measurement Procedure.....	19
<b>4 Results and Analysis.....</b>	<b>20</b>
4.1 Cantilever Deflection .....	20
4.2 Peltier Heating.....	21
4.3 Laser Heating .....	22
4.4 Programming Deflection with Uniform Pulses .....	23
4.5 Programming Deflection with Uniform Steps .....	25
<b>5 Conclusion and Future Work.....</b>	<b>28</b>
<b>6 References.....</b>	<b>29</b>
<b>7 Appendix A-VI Documentation.....</b>	<b>30</b>

## Table of Figures

Figure 2-1. DRAM Memory Cell. ....	6
Figure 2-2. VO <sub>2</sub> Hysteresis Curves.....	8
Figure 2-3. VO <sub>2</sub> temperature excursion. ....	9
Figure 2-4. Electro-Mechanical Memory Cell.....	11
Figure 3-1. XRD Scans of the test substrate, before and after the transition.....	13
Figure 3-2. Measurement Setup Schematic. ....	14
Figure 3-3. Final Setup. ....	15
Figure 3-4. Laser Modulating Circuit. ....	17
Figure 3-5. Measurement GUI.....	18
Figure 4-1. Side View of the 350 μm Cantilever (30° C and 90° C). ....	20
Figure 4-2. Deflection vs. Temperature (Peltier Heating). ....	21
Figure 4-3. Laser spot positions.....	22
Figure 4-4. Cantilever pulse transient response.....	23
Figure 4-5. Deflection with constant energy increase. ....	24
Figure 4-6. Step Size Unadjusted.....	25
Figure 4-7. Step Size Adjusted. ....	26
Figure 4-8. Deflection with constant steps. ....	27

# 1 Introduction

## 1.1 Motivation

The insulator-to-metal-transition (IMT) of 3-D (i.e. bulk crystals) VO<sub>2</sub> was first reported in 1959[1]. Nine years later, researchers observed a very similar behavior in 2-D (thin films) VO<sub>2</sub>[2], and less than 5 years ago in 1-D (nanowires) VO<sub>2</sub>[3]. The dynamical behavior of VO<sub>2</sub> is a combination of electrical (Mott) and lattice distortion or structural (Peierls) transitions, and therefore it is commonly referred to as a Mott-Peierls transition. Due to the strong electron-phonon interaction in VO<sub>2</sub>, it is very difficult to identify a dominant mechanism. Nevertheless, its potential for micrometer-sized transducers is revealed by the multiple empirical demonstrations that show that the solid-solid phase transition in VO<sub>2</sub> can be induced using different mechanisms and that abrupt changes in many of its properties are inherent to that transition. The actuation mechanisms include ultrafast optical radiation [4]; strain [5]; electric field [6]; and heating, which is the most studied actuation method. The structural and electronic changes in VO<sub>2</sub> during its transition cause the drastic changes of the material's electrical, mechanical, optical, and electromagnetic properties.

The use of VO<sub>2</sub> thin films, is currently being considered in solid-state-based tunable frequency resonators [7] and filters [8], and memristors [9], whereas its use in micrometer-sized transducers has been limited. However, recent results have demonstrated a drastic change on the mechanical properties of VO<sub>2</sub> films during its IMT [10], giving an extra functionality to VO<sub>2</sub> films that could be very beneficial for the development of MEMS-based sensors and actuators.

The device reported in this work combines the drastic changes in the mechanical properties of VO<sub>2</sub> with its memory capabilities for developing a micrometer-sized mechanical memory. The device consists of a simple VO<sub>2</sub>-coated silicon cantilever, and the actuation was achieved by thermal heating from a laser diode. The work builds on results obtained for optoelectronic and all-optical multiple states in vanadium dioxide [11], and expands further the multifunctional memory aspect of this material. Furthermore, it demonstrates that controlled laser pulses can be used as the programming action.

In monolithically integrated MEMS, the heating by direct conduction would require the inclusion of a micro-heater in the MEMS design. The increase in temperature generated by these micro-heaters is caused by an electrical current flowing through a micro-meter sized conductive line (i.e. Joule heating) [12, 13]. In this work a cantilever is heated by a laser diode in order to study the effects of localized heating. By using a laser, the area being heated can be modified and controlled without having to redesign the cantilever. Also, by using a laser to heat the cantilever, the measurement and actuation setup is simplified.

Other steps towards the characterization of our system where: 1. to determine the full scale operating range of the bimorph cantilever tip displacement, 2. to experimentally find the minimum energies required to program distinguishable displacement states in the mechanical memory, 3. to demonstrate repeatability and control in achieving the different states, and 4. To measure the stability of each state and it's sensitivity to temperature.

## 1.2 Literature Review

In 1834 the first analytical machine was designed by Babbage. It was a fully mechanical system capable of calculating polynomials with great precision. The numbers were stored in columns of rotating wheels [14]. This idea of storing and manipulating data in a mechanical way evolved with time, and was of great impact at the time. But when the transistor was invented, there was a huge shift in how computation machines were designed. At the time mechanical parts were large, slow and required more power than their electronic counterparts. Therefore, mechanical switches were replaced by transistors, and storage elements were replaced by capacitors and inductors. For many years this has become the standard, and devices have become smaller and faster. But thanks to the development of newer technologies like Micro-Electro Mechanical Systems (MEMS), mechanical systems no longer have to be big and slow. Mechanical parts can now be built in the micro-meter ( $\mu\text{m}$ ) or even nano-meter (nm) range.

Recently, a research group lead by Christian Joachim from the A\*STAR Institute of Materials Research and Engineering in Singapore built a molecule-size gear capable of full rotation in both directions [15]. These advances have improved the performance of mechanical systems to the point where they can now compete with their electrical counterparts. MEMS switches provide ultra-low losses, high isolation, highly linear relays, and they can be designed to operate within a broad spectrum of frequency (i.e., they can operate over a wide frequency range). They can also be fabricated using the same technology used in integrated circuit (IC) fabrication. These advances have allowed the development mechanical computational systems with the speed and efficiency of electronic circuits.

In almost all computational systems, there is the necessity to store information in some sort of memory module for later retrieval. These memory modules have been implemented as electronic devices in many different varieties, such as RAM, ROM, DRAM, EEPROM, etc. These fully electronic memories suffer from some deficiencies that new electro-mechanical memories might be able to solve.

### **1.3 Summary of the Following Chapters**

Chapter 2 will give a brief background on the evolution of mechanical memories and it will explain important concepts and general terminology used when dealing with any type of memory. It will also explain how vanadium dioxide is a useful material that can be used in the creation of electrical, optical, and mechanical memories. Finally it will discuss a possible implementation of an electro-mechanical memory, using vanadium dioxide. Chapter 3 will discuss the deposition and subsequent analysis of the VO<sub>2</sub> film. It will also discuss the details of the measurement setup, control circuit, and computer graphical user interface. It will also discuss the experimental procedure. The results obtained in the experiments are presented in chapter 4 and conclusions are presented in chapter 5.

## 2 Theoretical Background

### 2.1 “Memory” Concepts

There are various concepts that must be understood when dealing with memory devices. When we store information in a memory device, it is not only important to be able to store and retrieve that information (data), but it is also important to know where it is. The smallest unit where the information is stored is known as the “memory cell”. The location of the cell is known as the “address”. When it comes to addressing data, there are basically two types of memories, Random Access Memory and Sequential Access Memory. In the Random Access Memory, it is possible to go directly to any address and read the data, while Sequential Access Memory the data must be read in certain order without skipping. The process of storing a piece of data to a memory device is called writing, and the process of retrieving data is called reading. Some devices, once written, cannot be re-written. These memory devices are known as Read Only Memory (ROM). An example of a ROM memory is music Compact Disc (CD). A memory device that can be read and written is known as a Read-Write Memory (RW), for example a computer hard drive. Another characteristic that is very important in memory devices is its volatility. This refers to the memory’s ability to store data permanently. A memory device that requires power in order to preserve the stored data and would otherwise lose all the data is known as a volatile memory. A memory device that can store data permanently, even when it loses power is known as a non-volatile memory. So far, no distinction has been made about the data that is being written. This can be analog values such as in an audio cassette, digital values such as in a computer memory

module, or even a combination as in multiple discrete states. Each type of data type has its own advantages and can be stored in different ways.

## 2.2 A Simple Electronic Memory Cell

There are many ways of implementing a fully electronic memory device. (Figure 2-1) shows an example of a DRAM memory cell. DRAM is chosen because it is the closest analog to current designs of micro electro-mechanical memories.

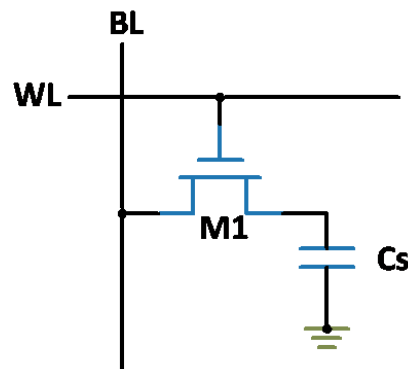


Figure 2-1. DRAM Memory Cell.

The main storage element is the capacitor “Cs”. Binary data is stored as a voltage in this capacitor. The capacitor can be charged --which represents a logical “1” or high state value--, or it can be uncharged --which represents a logical “0” or low state value. The capacitor is connected to the read/write circuit through the switch “M1” which is implemented as a MOSFET transistor<sup>1</sup>. The device is addressed through the “Word Line” (WL) and the “Bit Line” (BL).

---

<sup>1</sup>An enhancement mode transistor is assumed in this case, since otherwise the capacitor Cs will always be connected to BL until a voltage is applied.

When the WL is connected to a voltage with magnitude higher than the transistor's threshold<sup>2</sup>, the switch M1 will be "on", allowing the charging of capacitor Cs with the voltage at the BL node. The voltage of the capacitor can be read or written. When the capacitor is read it is discharged at the same time, which destroys the information. This requires the value to be re-written after each read. Another problem with this type of memory is that the switch is not perfect and there is charge leakage from the capacitor which requires periodic refreshing of the data. Many attempts have been made for improving the performance of these cells, including different storage capacitor designs, and MOSFET designs with low current leakage (which can be achieved by controlling the reverse saturation current of the reversed bias junction formed at the transistor's drain). This memory is classified as a RW Dynamic Random Access Memory (DRAM).

## 2.3 The Use of VO<sub>2</sub> in Memory Devices

Vanadium Dioxide (VO<sub>2</sub>) exhibits a well-known insulator-to-metal transition during which several of its physical properties change significantly. A hysteresis loop develops for each of them as the material is heated and then cooled through the transition. The transition temperature is usually at around 68°C. (Figure 2-2) shows how the resistance of a sample of VO<sub>2</sub> changes during the transition. It can be seen that the resistance changes more than two orders in magnitude. These drastic changes in the materials properties lend themselves to applications in electrical and optical switching devices. Most importantly for this work, the hysteresis allows for the creation of memory devices.

---

<sup>2</sup>The magnitude and polarity of the transistor's threshold voltage will be determined by the type of transistor (PMOS or NMOS).

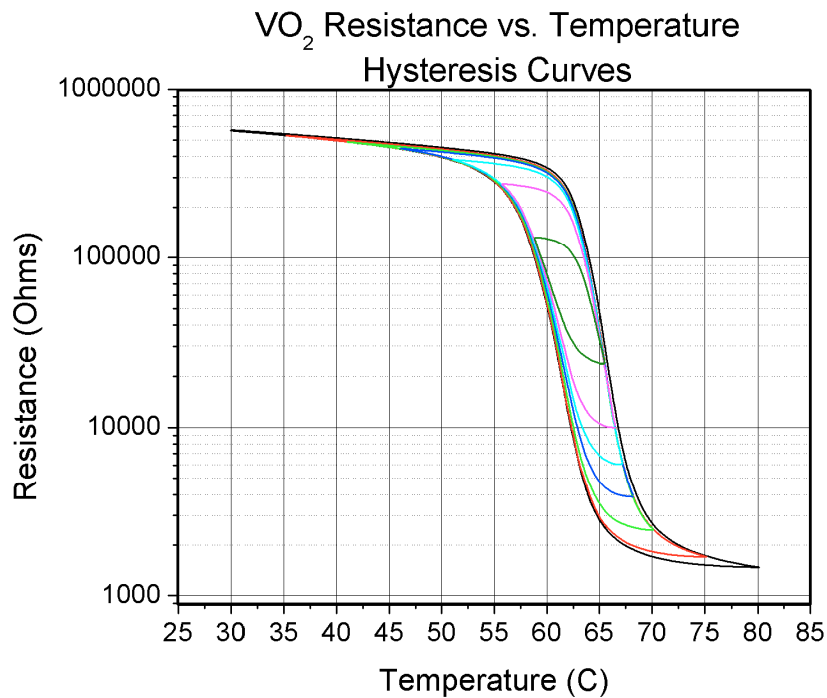


Figure 2-2. VO<sub>2</sub> Hysteresis Curves.

To illustrate this memory capability, consider that the sample is originally at 30°C, and is now heated to 64°C. According to the hysteresis curves the resistance should be close to 100 kΩ. As long as the temperature remains constant, the resistance will remain at the same value. Now, if the sample is temporarily heated to 69°C and then allowed to cool back down to 64°C, the sample would have a new resistance value close to 10 KΩ. This heating process could be done by conductive heating from a Peltier heater or by light irradiation from a laser.

(Figure 2-3) shows the change in resistance of the VO<sub>2</sub> thin film as the temperature changes, and the scenario where a light pulse of 1s was applied. For the same temperature of 64°C the VO<sub>2</sub> film has two different values of resistance. The actual resistance value of the material will depend on the history of the temperature changes. In this sense, the material “remembers” the

past inputs. If a light pulse of different magnitude and/or different duration was applied, the resistance would have followed a different path. In this case, assuming that the laser pulse was applied at the same “place” as before (marked in Figure 2-3 as “Start of Pulse”), the resistance excursion would have followed the same decreasing curve shown, since this curve defines the rightmost limit boundary of the hysteresis. However, the monotonic decrease in resistance would have stopped at a different resistance value (and so would the returning curve connected to this low resistance value). This behavior occurs with all of the properties that change during the transition. Since the material’s transition is caused by heat, the transition can also be initiated by Joule heating from an electrical pulse. In that way, this material can be used to create fully electrical memories, fully optical memories or a combination of both.

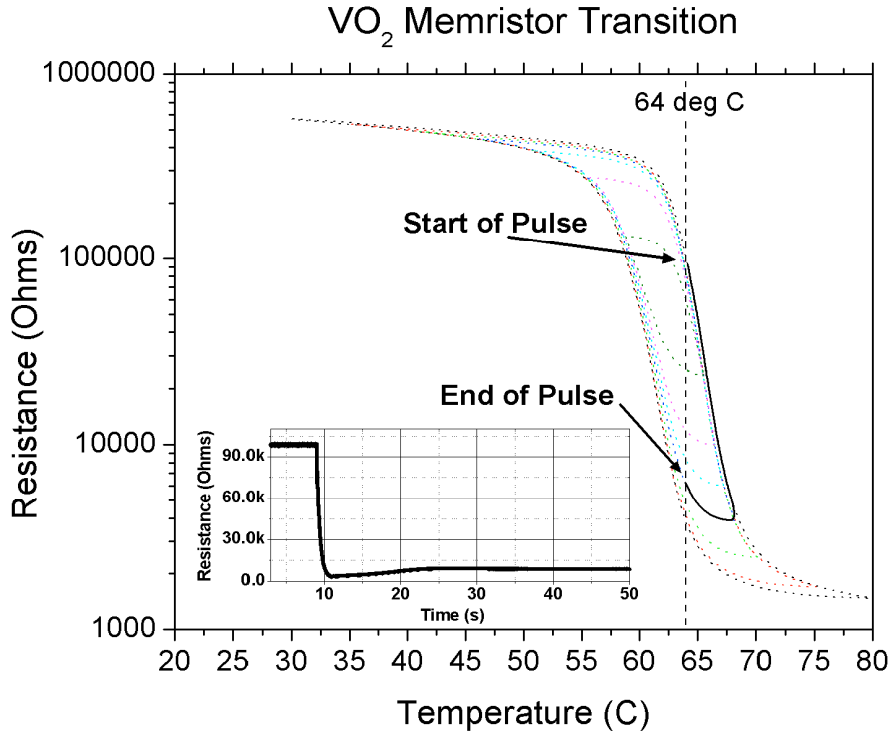
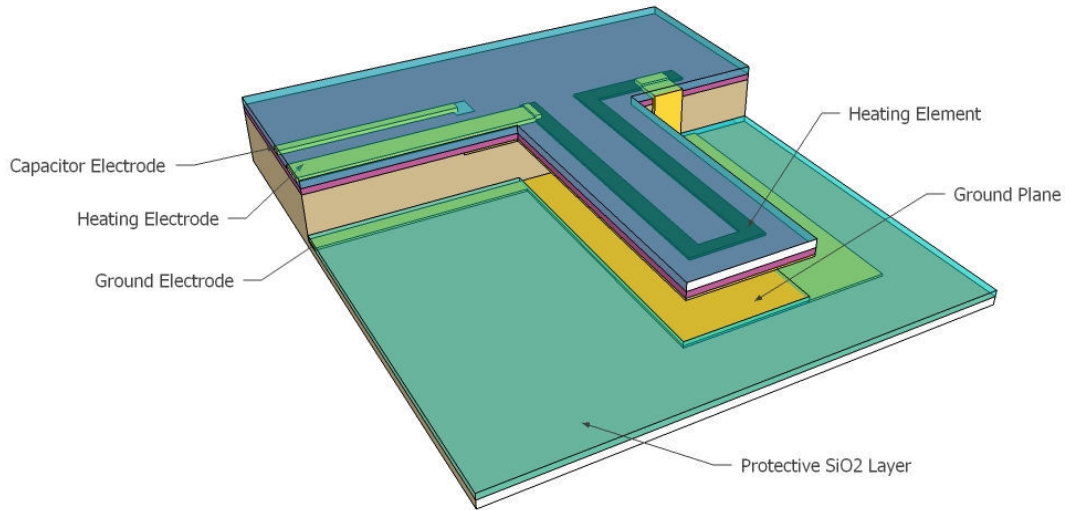


Figure 2-3. VO<sub>2</sub> temperature excursion.

Of interest in this work are the high reversible strains that develop in  $\text{VO}_2/\text{Si}$  cantilevers. These strains cause the cantilever to bend as the materials goes through its transition. This bending has the same hysteretic behavior that the other properties have and can be potentially used to implement an electromechanical memory.

## 2.4 Possible $\text{VO}_2$ Based Electro-Mechanical Memory

(Figure 2-4) shows a possible implementation of an electro-mechanical memory cell. It consists of a high resistivity silicon (Si) cantilever with a heating element on its top surface. There is a second electrode on the substrate surface forming a capacitor. All connections are routed to the left in the figure. The entire cell is coated with a protective layer of  $\text{SiO}_2$ . This coating will isolate the electrodes and heating element from the  $\text{VO}_2$  thin film. The  $\text{VO}_2$  film deposition would be the final step; it would be deposited over the entire array and would not need to be patterned. The entire array would be placed in a temperature controlled environment. Cantilever deflection would be measured as a change in capacitance. This capacitance can be read in many ways. If the capacitor is charged with a DC voltage, the electrostatic force might cause errors when reading the deflection. Therefore, a possible solution might be to apply a purely AC signal and measuring the impedance. The cantilever will oscillate slightly around its average deflection. Writing a value to the cell would consist of sending an electrical pulse through the heating electrode. This will cause a bending in the cantilever which could be read by measuring the capacitance from the capacitor electrode to ground. It should be possible to write different values of deflection to the cantilever by controlling the energy of the electrical pulse.



**Figure 2-4. Electro-Mechanical Memory Cell.**

The purpose of this work is to examine the potential use of  $\text{VO}_2$  coated Si cantilevers in the implementation of an electro-mechanical memory based on the deflection of the cantilever. Since it is only of interest in this work to study the ability of the  $\text{VO}_2/\text{Si}$  cantilever to store a value of deflection, the cantilever will be heated with a laser pulse instead of an electrical pulse. It is expected that the behavior will remain the same for the case of Joule heating. The deflection will be measured using laser deflection techniques and an optical setup.

## 3 Materials and Methods

### 3.1 Silicon Micro-Cantilevers and VO<sub>2</sub> Deposition

VO<sub>2</sub> thin films were grown by pulsed laser deposition (PLD) on commercially available silicon micro cantilever chips (MikroMasch) and on companion test substrates. As specified by the manufacturer, the cantilever used for the detailed measurements had length, width, and thickness of, respectively, 350, 35, and 1 μm, and a spring constant of ~0.6 N/m. A krypton fluoride excimer ( $\lambda=248$  nm) laser with fluence 4 J /cm<sup>2</sup>, pulse duration ~20 ns, and repetition rate of 10 Hz was used for ablation of a vanadium metal target. The PLD process was performed in vacuum chamber in an oxygen/argon atmosphere with a background pressure of 20 μTorr. Total gas pressure was 50 mTorr during depositions and substrate temperature was kept constant at T=550°C. Film thickness was 300 nm, as measured with a stylus profilometer on reference steps created on the cantilever chip. (Figure 3-1) shows X-ray diffraction (XRD) scans that were performed on the test substrates. They show that the films are polycrystalline and strongly oriented with the monoclinic (011)<sub>M</sub> planes parallel to the substrate surface. When heated through the IMT, film structure changes reversibly to the tetragonal R phase, and the (110)<sub>R</sub> planes are then parallel to the surface. The room temperature XRD scans were also used to approximate the average crystallite size ( $\tau$ ) of the VO<sub>2</sub> film in the monoclinic region by using the Scherrer equation:

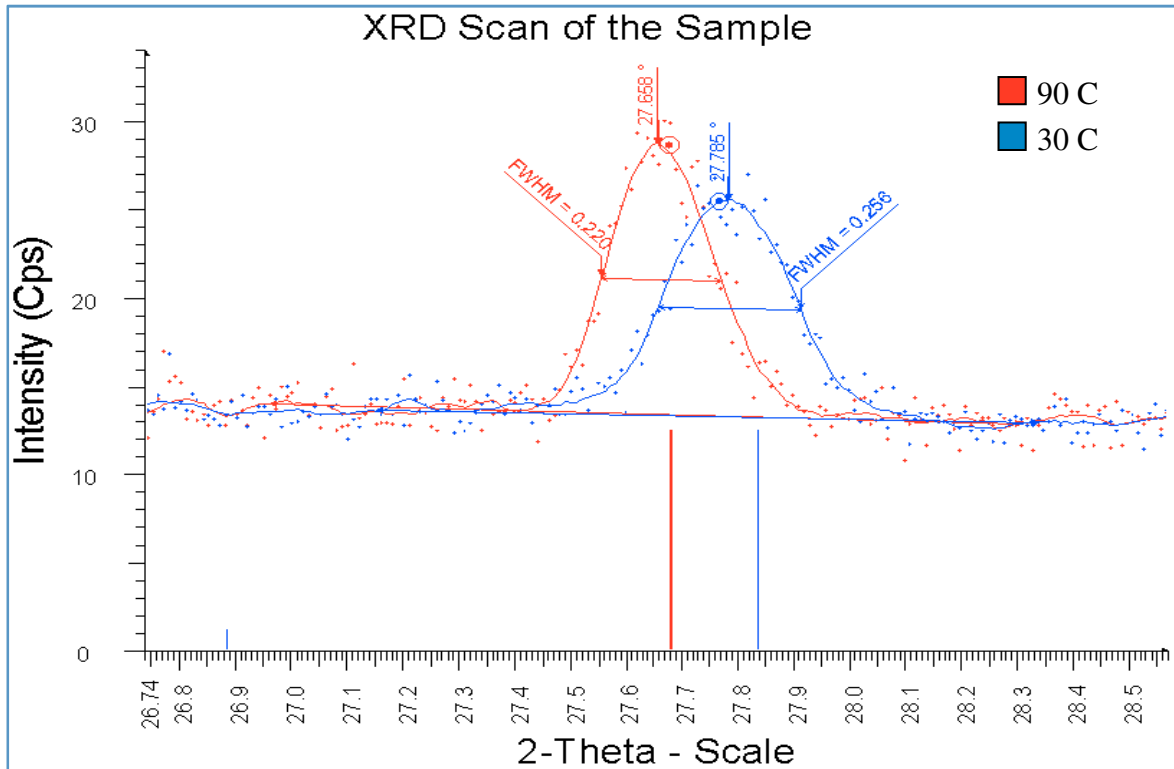


Figure 3-1. XRD Scans of the test substrate, before and after the transition.

$$\tau = \frac{K\lambda}{B\cos(\theta)}$$

where  $\lambda$  is the wavelength of X-ray,  $B$  is the breadth of the X-ray beam at half the maximum peak intensity (i.e. full width at half maximum, or FWHM),  $\theta$  is the angle that satisfies the Bragg condition, and  $K$  is the Scherrer constant (assumed to be 0.9 in the present case). The measured values for  $B$ , and  $\theta$ , were  $4.537 \cdot 10^{-3}$  and  $27.785^\circ$  respectively. Therefore, the estimated crystallite size of the  $\text{VO}_2$  film in the monoclinic region was 35 nm. Both peaks are slightly shifted to the left of the strain free peak locations, suggesting that the film is under compressive stress. The Mott-Peierls transition that the  $\text{VO}_2$  experiences causes the structural change responsible for the deformation of the cantilevers.

## 3.2 Measurement System and Procedure

### 3.2.1 Measurement System

(Figure 3-2) shows a schematic of the experimental setup. The final setup can be seen in (Figure 3-3). In this setup a laser (L1), is focused and aimed at the tip of the bimorph cantilever. This laser was used to measure the deflection of the cantilever beams. L1 has a wavelength of 672 nm and the intensity was set to around  $500 \mu\text{W}$  so that the intensity does not affect the cantilever.

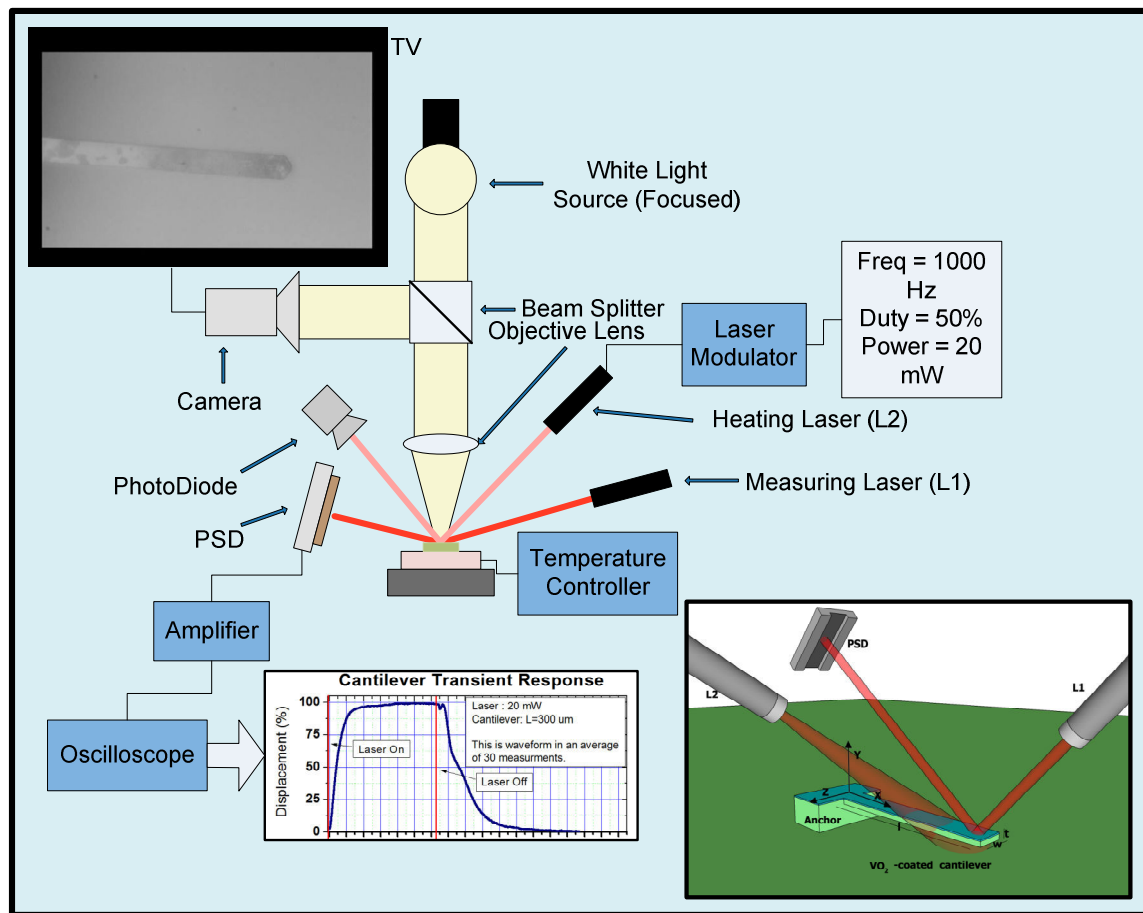
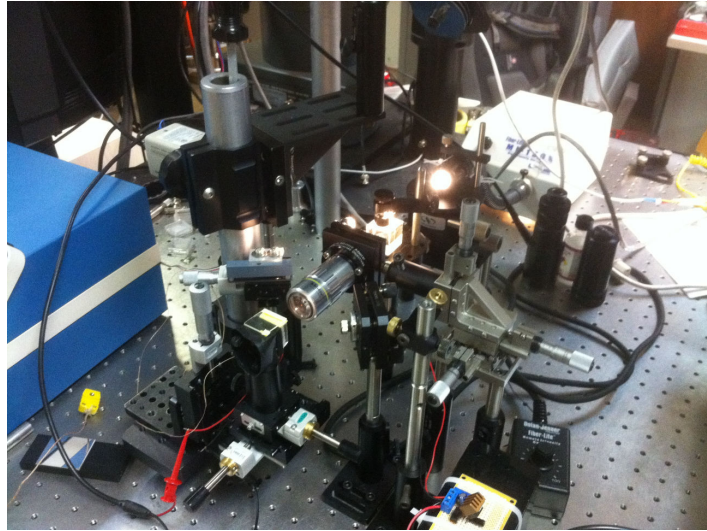


Figure 3-2. Measurement Setup Schematic.



**Figure 3-3. Final Setup.**

The reflected beam is then aimed at a position sensitive detector (PSD) (Hamamatsu S3270). As the cantilever moves the PSD will produce a voltage proportional to displacement. The second laser (L2) also has a wavelength of 672 nm, but it had a wider beam spot size in order to cover the entire width of the cantilever, and the intensity was adjusted to heat the cantilever. The intensity of the lasers were measured with an optical power meter (Thorlabs model: PM100D). These two lasers are actually arranged orthogonal to each other so that the light from L2 does not affect the PSD reading, which relates only to the beam reflected from L1. The voltage of the PSD is amplified by a DC coupled amplifier and filtered for HF interference. The cantilever movement will ultimately be caused by photo-thermally induced heat, as generated from laser L2. The power output of this laser is adjusted until the temperature of the cantilever rises beyond 80 °C. This is determined by observing the deflection and raising the power until the deflection saturates. This power output will be set as the maximum laser power in the experiments. It's important to be able to see the top of the cantilever in order to correctly focus the two laser

beams. Normally, a microscope would be needed, but the microscope objective lens would make it practically impossible to focus the two lasers without hitting the lens. For that reason, an objective lens with a much larger focal length is used and a beam splitter is used in order to “feed in” enough white light. The entire setup is constructed on an optics air-suspended table in order to reduce vibrations. When measuring the “memory” properties of the system, the cantilever needs to be at an average temperature close to the start of the IMT region, so that a small energy input causes a measurable response. In order to accomplish this, a Peltier heater (Custom Thermoelectric 03111-9L31-04CG) was used along with a PID temperature controller. Also, in order to control the induced heat from the laser, a computer controlled modulating circuit shown in (Figure 3-4) was built. This circuit, if built as shown will modulate a laser diode with a square wave with adjustable intensity, duty cycle, and frequency, while at the same time protecting the diode from transient over-voltages and excessive currents. The circuit is accompanied by a sub circuit that produces +12V, +5V, -5V from a single 12V supply.

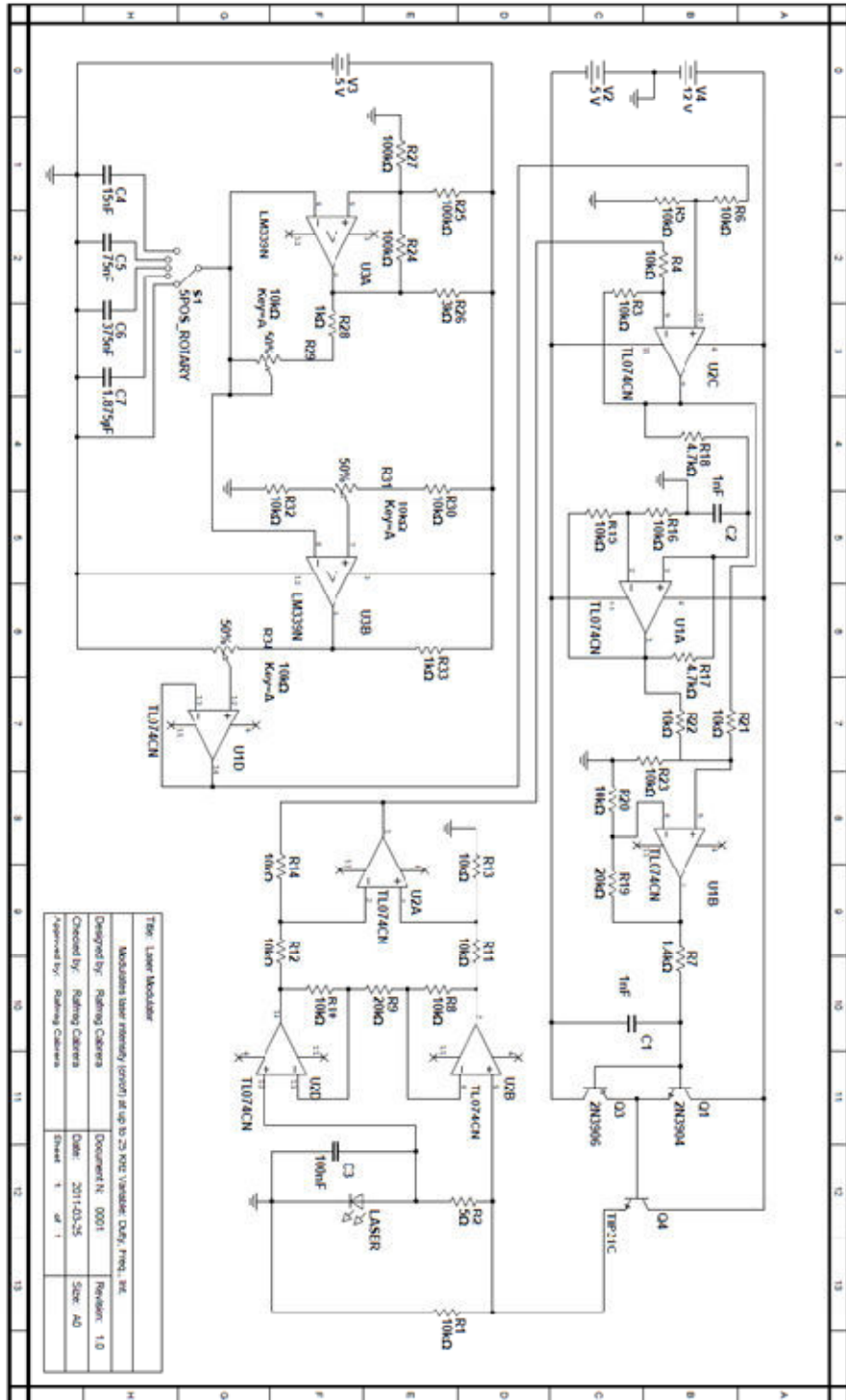


Figure 3-4. Laser Modulating Circuit.

If the connection to pin 12 of OpAmp U1D in the circuit is disconnected, and that pin is connected to a computer controlled 0-5 V signal, the laser can be controlled by that computer. The signals from the temperature controller and PSD were connected to a computer. The entire set-up was computer-controlled. LabVIEW software was used to implement a graphical user interface (GUI) that would facilitate the control and data acquisition of the experiments. The front panel of this GUI is shown in (Figure 3-5).

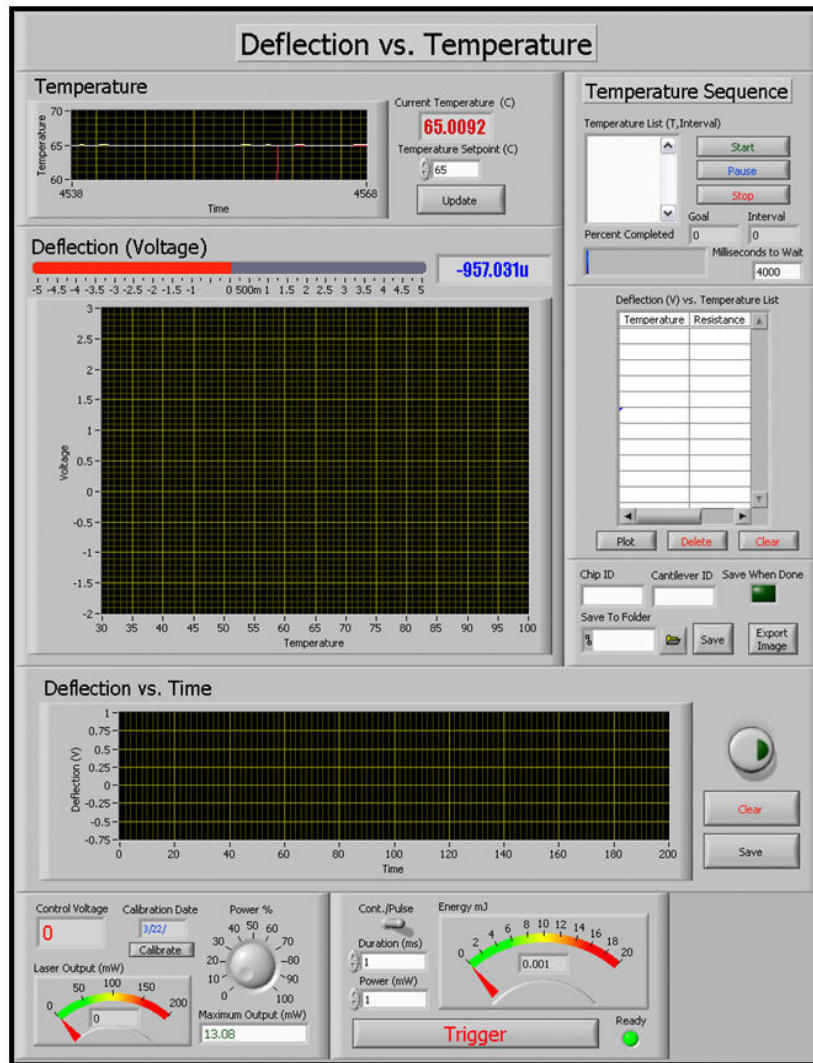


Figure 3-5. Measurement GUI.

This program performs automated temperature sweeps while plotting the deflection. It also allows manual control of the temperature and laser intensity, and saves the transient response of the cantilever as detected from Laser L1, while it is excited by the laser pulses from L2. All of the data can be exported as a CSV file.

### **3.2.2 *Measurement Procedure***

The experiment will consist of the following:

1. Use a microscope in combination with a Lasico Fillar Eyepice to measure the minimum and maximum displacement in order to calibrate the voltage measurement from the PSD.
2. Measure the cantilever displacement vs. temperature to determine the maximum and minimum deflection values to calibrate the output of the PSD.
3. Measure the response of the cantilever to pulses of varying energy in order to characterize the behavior.
4. Determine the relationship between pulse energy and cantilever deflection.
5. Demonstrate control of the changes in deflection.

## 4 Results and Analysis

### 4.1 Cantilever Deflection

After mounting the cantilever in the microscope, side-view photographs of the cantilever were taken at 30° C and at 90° C. (Figure 4-1) shows a side-view composite image of the cantilever. The minimum and maximum deflections were measured to be -22  $\mu\text{m}$  and -2  $\mu\text{m}$  respectively. 0  $\mu\text{m}$  deflection is when the cantilever is perfectly flat; the negative implies that the cantilever is bent downward. This corresponds to the film being in compressive stress as seen in the XRD data. Because the heating of the measuring laser (L1) was negligible, it was assumed that the minimum and maximum displacement obtained while heating under the microscope are the same as when measured in the final setup. The 350  $\mu\text{m}$  cantilever was chosen for the rest of the experiment due to the fact that it produced the largest deflections (best measurable response). These deflections are much larger than those obtained from thermal expansion-based bimorph cantilevers.



Figure 4-1. Side View of the 350  $\mu\text{m}$  Cantilever (30° C and 90° C).

## 4.2 Peltier Heating

The sample was mounted on the measurement setup and the deflection was measured as the temperature was swept from 30°C to 100°C and back. (Figure 4-2) shows the PSD output voltage as the temperature was varied. This voltage is proportional to the cantilever deflection. The red line shows the deflection as the sample is heated and the blue line shows the deflection as the sample is cooled down. The hysteresis is about 30° C wide. The PSD voltage at 30°C and at 100°C corresponds to the minimum and maximum deflection. Since the relationship is linear, a conversion from PSD voltage to deflection can be calculated.

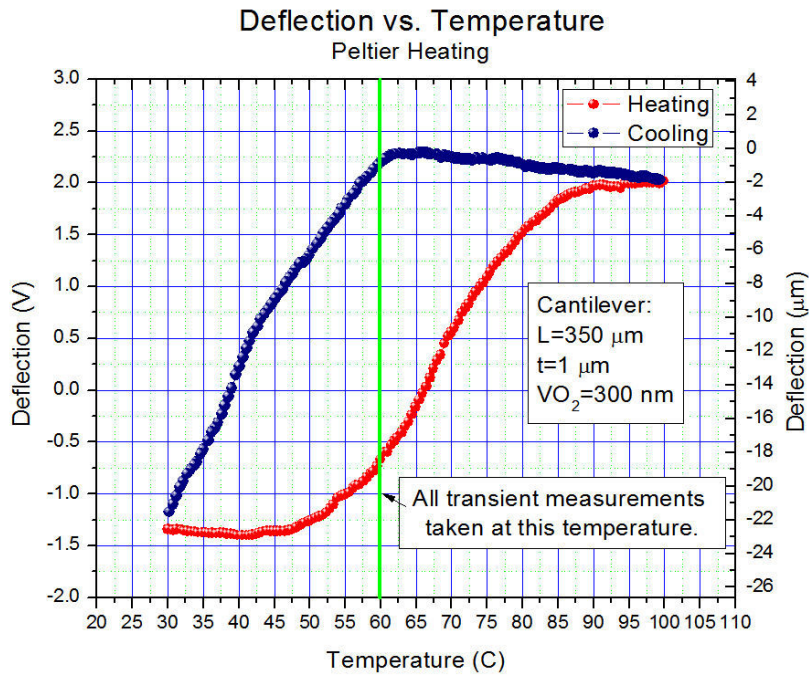


Figure 4-2. Deflection vs. Temperature (Peltier Heating).

$$Deflection = 6.15 * Voltage - 14.31 \quad (\mu m)$$

The operating temperature was chosen to be 60°C because it is at this temperature that the biggest difference between the heating and cooling curves was observed. In other words, it was in this region that the largest change in deflection was expected.

### 4.3 Laser Heating

The heating laser was focused to a spot of about 100 μm and centered on the cantilever while the measuring laser was focused to a spot of about 35 μm and aimed at the tip of the cantilever; see (Figure 4-3). This configuration was used for all of the measurements.

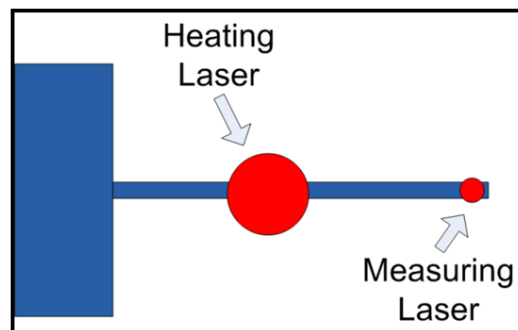


Figure 4-3. Laser spot positions.

In order to analyze the transient response of the cantilever, the heating laser was modulated by a 50% duty cycle square wave. 30 cycles were averaged and the result is shown in (Figure 4-4). These measurements were taken with the setup at room temperature. As can be seen in Figure 4-4 by analyzing the time constant, the response is limited to around 200 Hz. Contrary to when the sample was heated with a Peltier heater, the deformation does not have a uniquely defined radius

of curvature, since the position and size of the heating laser spot affects the final shape of the cantilever. The optimum position and size of the heating laser spot was found empirically.

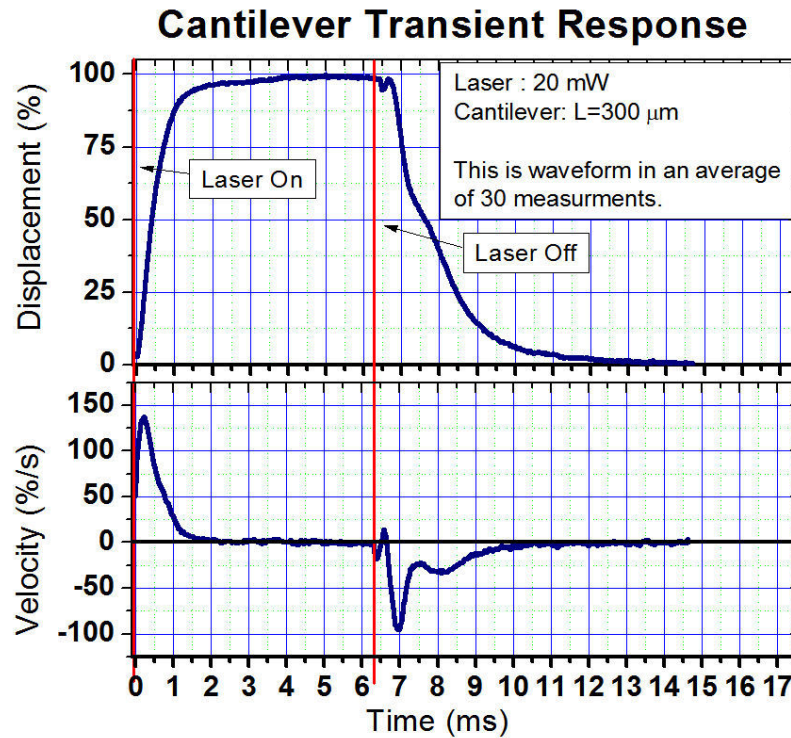


Figure 4-4. Cantilever pulse transient response.

#### 4.4 Programming Deflection with Uniform Pulses

Before every run the sample was “reset”. This consisted of raising the temperature to 100°C and then lowering it to 30°C. This guaranteed the same starting point for every experiment. Then, the sample was raised to the working temperature of 60°C. The cantilever was then exposed to 1ms pulses of varying intensity. The total energy was increased by a constant amount of 1 μJ starting with 1μJ. the resulting deflection is shown as the black trace in (Figure 4-5). As can be seen,

with every pulse the deflection changed by a small amount and remained at that amount until the next pulse. The cantilever would hold this “state” of deflection as long as the temperature of the Peltier heater remained constant at 60°C.

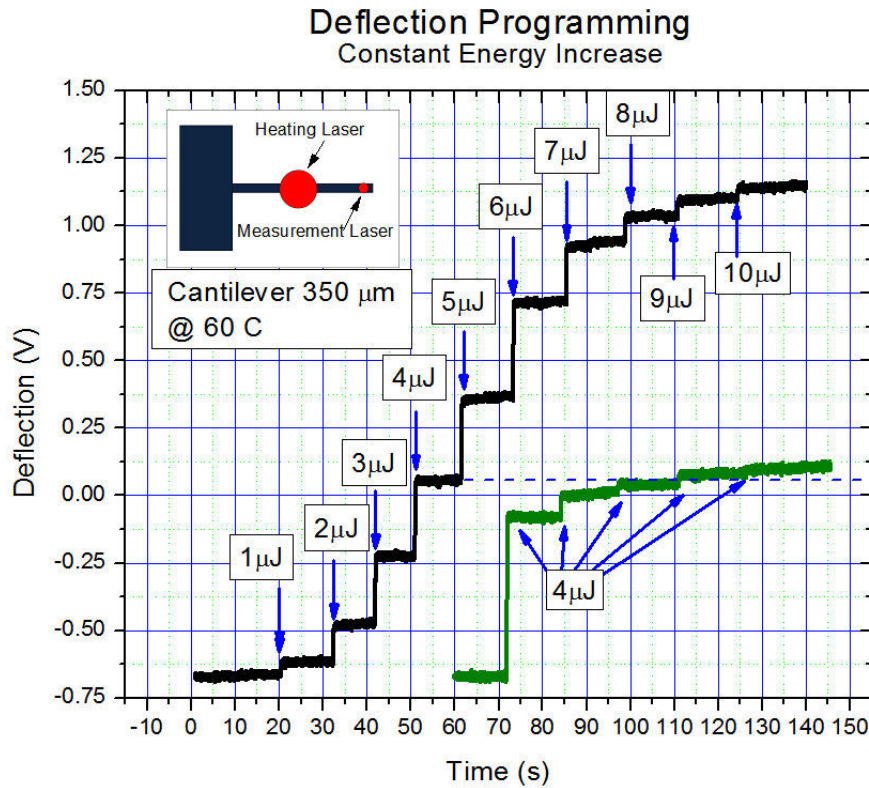


Figure 4-5. Deflection with constant energy increase.

After these measurements, the cantilever was “reset” for the next experiment, which consisted on exposure to multiple pulses of the same amount of energy. This is shown as the green trace in (Figure 4-5). This observation suggests the final value of deflection will depend mainly on the amount of energy of the pulse. It can also be seen that the change in deflection for each pulse is not a linear relationship with the increase in energy for each pulse. It seems that the change in

deflection is a function of the current deflection and the increase in energy of the pulse. This information was used to adjust the increase in energy for each pulse, in order to get a more uniform increase in steps of deflection.

## 4.5 Programming Deflection with Uniform Steps

In order to determine the relationship between the step size and pulse energy, the step size is plotted as a function of pulse number. This is shown in (Figure 4-6). It can be noticed that the step size varies significantly. An arbitrary goal step size was chosen, 0.139 V. this is shown as a blue line in (Figure 4-6).

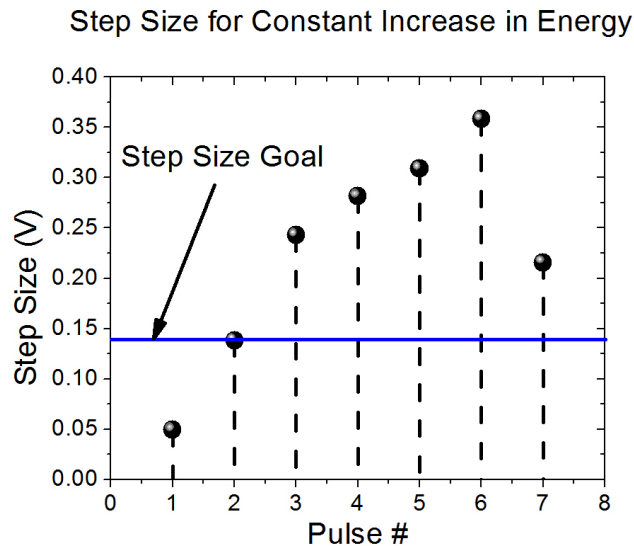
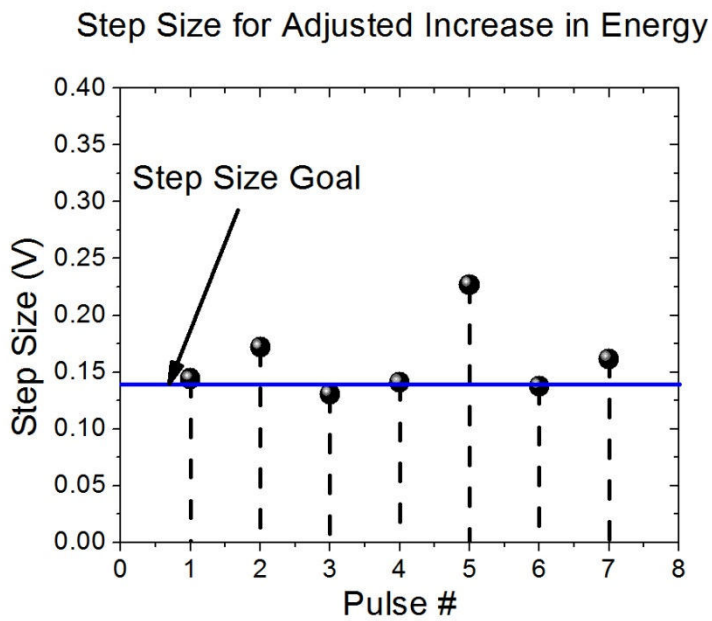


Figure 4-6. Step Size Unadjusted.

For each pulse, the ratio of goal step to measured step is calculated. It is assumed that this ratio is the same factor by which the energy change for that step needs to be either increased or decreased. After modifying the energy increases, a new sequence of energy pulses was

calculated. The sample was reset and the new sequence was applied. (Figure 4-7) shows the new distribution of step sizes for each pulse. As can be seen much better uniformity was achieved for the step size. This also allows for more uniform “mechanical memory states”. Finally, (Figure 4-8) shows the final performance of the programmable mechanical memory. Each step was held for approximately 20 s. The inset shows the final pulse energy sequence.



**Figure 4-7. Step Size Adjusted.**

### Deflection Programming Adjusted Energy

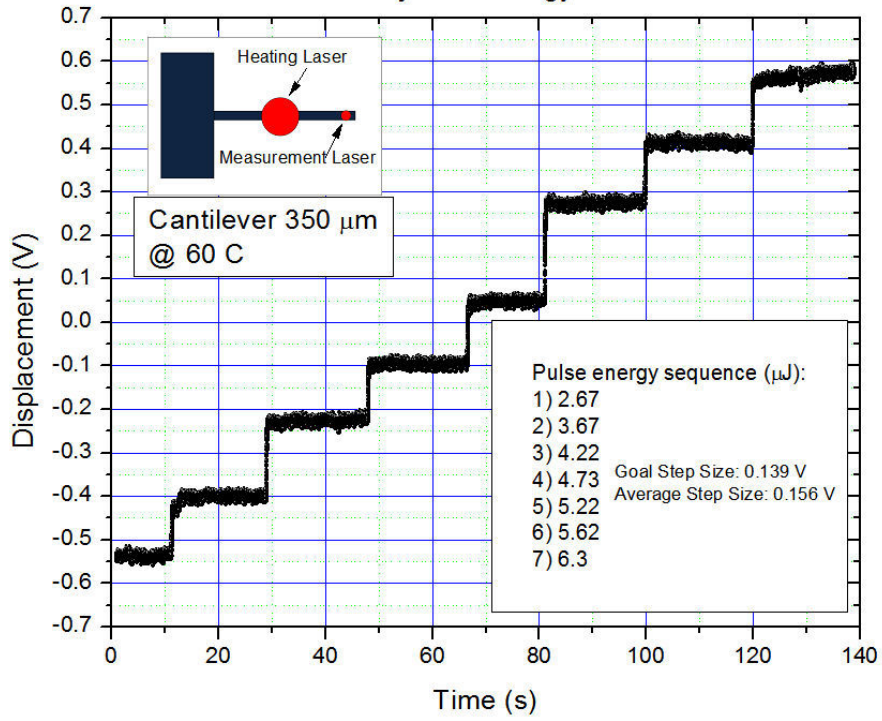


Figure 4-8. Deflection with constant steps.

## 5 Conclusions and Future Work

A multiple state mechanical memory was implemented and tested. Absolute displacements up to 21  $\mu\text{m}$  were achieved. The resulting states were stable and fully programmable. The device is highly sensitive to temperature variations and therefore the long-term volatility of the memory was not tested due to the setup's limitations.

The amount of energy needed to actuate the cantilever was found to be a few  $\mu\text{J}$  which is promising for future implementation in integrated devices. The response time of the cantilever due to a light pulse was found to be in the millisecond range which is comparable to the writing limitations in some current electronic memories. Vanadium Dioxide was shown to be a useful material in the design of novel electromechanical memories.

Future work might include the design of a full monolithic memory array with the necessary decoding and interface circuits. The system's high sensitivity to temperature variations is still a big limitation. Future work might also include research into the fabrication of  $\text{VO}_2$  thin films in order to shift the transition temperature closer to room temperature and to widen the hysteresis. Both of these effects would largely improve the performance of a  $\text{VO}_2$ -based memory device.

## 6 References

- [1] F. J. Morin, "Oxides Which Show a Metal-to-Insulator Transition at the Neel Temperature," *Physical Review Letters*, vol. 3, p. 34, 1959.
- [2] G. A. Rozgonyi and D. H. Hensler, "Structural and Electrical Properties of Vanadium Dioxide Thin Films," *Journal of Vacuum Science and Technology*, vol. 5, pp. 194-199, 1968.
- [3] S. Choi, *et al.*, "Synthesis of VO<sub>2</sub> Nanowire and Observation of Metal-Insulator Transition," *Japanese Journal of Applied Physics*, vol. 47, p. 3296.
- [4] A. Cavalleri, *et al.*, "Femtosecond Structural Dynamics in VO<sub>2</sub> during an Ultrafast Solid-Solid Phase Transition," *Physical Review Letters*, vol. 87, p. 237401, 2001.
- [5] CaoJ, *et al.*, "Strain engineering and one-dimensional organization of metal-insulator domains in single-crystal vanadium dioxide beams," *Nat Nano*, vol. 4, pp. 732-737, 2009.
- [6] B.-G. Chae, *et al.*, "Abrupt metal-insulator transition observed in VO<sub>2</sub> thin films induced by a switching voltage pulse," *Physica B: Condensed Matter*, vol. 369, pp. 76-80, 2005.
- [7] M. J. Dicken, *et al.*, "Frequency tunable near-infrared metamaterials based on VO<sub>2</sub> phase transition," *Opt. Express*, vol. 17, pp. 18330-18339, 2009.
- [8] J. Givernaud, *et al.*, "Tunable band stop filters based on Metal-Insulator Transition in vanadium dioxide thin films," in *Microwave Symposium Digest, 2008 IEEE MTT-S International*, 2008, pp. 1103-1106.
- [9] T. Driscoll, *et al.*, "Phase-transition driven memristive system," *Applied Physics Letters*, vol. 95, pp. 043503-3, 2009.
- [10] A. Rua, *et al.*, "Bending in VO<sub>2</sub>-coated microcantilevers suitable for thermally activated actuators," *Journal of Applied Physics*, vol. 107, pp. 074506-4, 2010.
- [11] H. Coy, *et al.*, "Optoelectronic and all-optical multiple memory states in vanadium dioxide," *Journal of Applied Physics*, vol. 108, pp. 113115-113115-6, 2010.
- [12] M. Einat and M. Grajower, "Microboiling Measurements of Thermal-Inkjet Heaters," *Microelectromechanical Systems, Journal of*, vol. 19, pp. 391-395, 2010.
- [13] G.-S. Chung and J.-M. Jeong, "Fabrication of micro heaters on polycrystalline 3C-SiC suspended membranes for gas sensors and their characteristics," *Microelectronic Engineering*, vol. 87, pp. 2348-2352, 2010.
- [14] A. G. Bromley, "The evolution of Babbage's calculating engines," *IEEE Ann. Hist. Comput.*, vol. 9, pp. 113-136, 1987.
- [15] C. Manzano, *et al.*, "Step-by-step rotation of a molecule-gear mounted on an atomic-scale axis," *Nat Mater*, vol. 8, pp. 576-579, 2009.

## **7 Appendix A-VI Documentation**



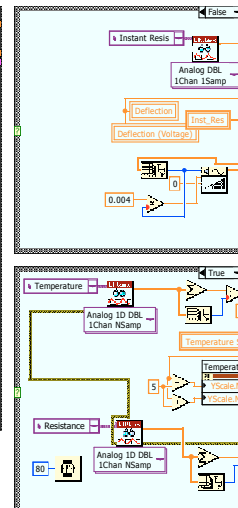
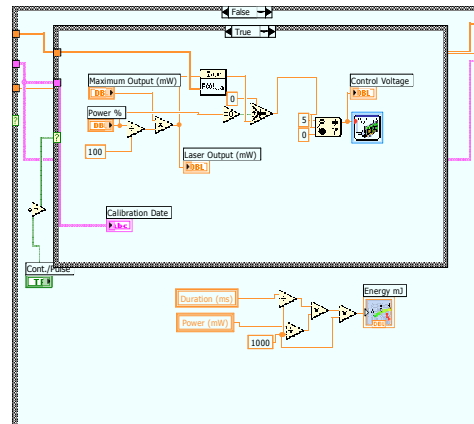
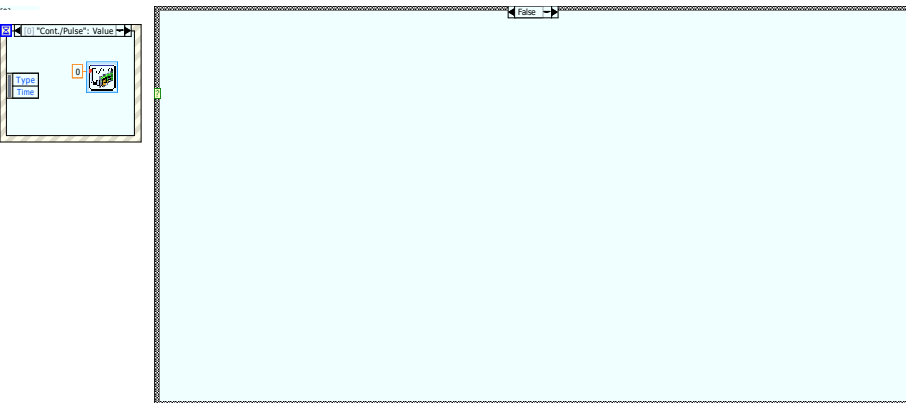
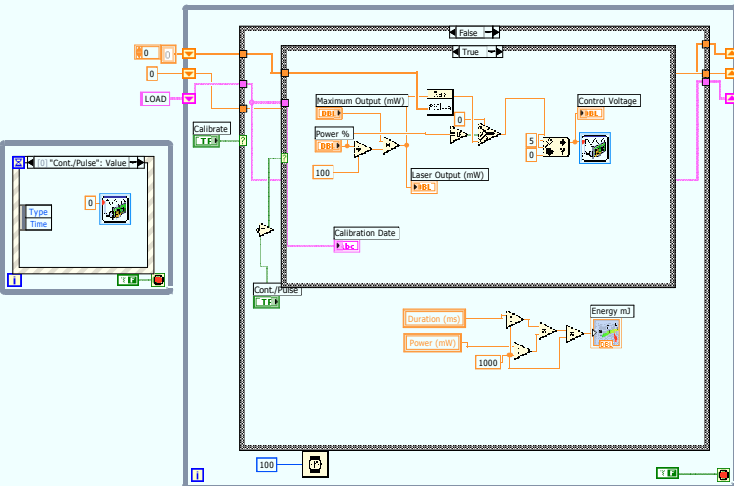
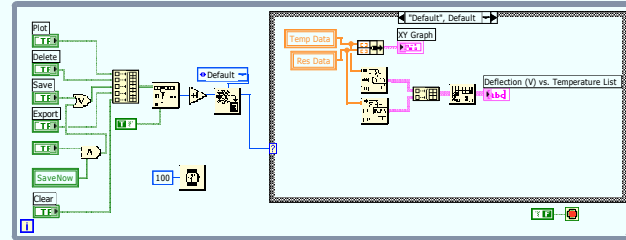
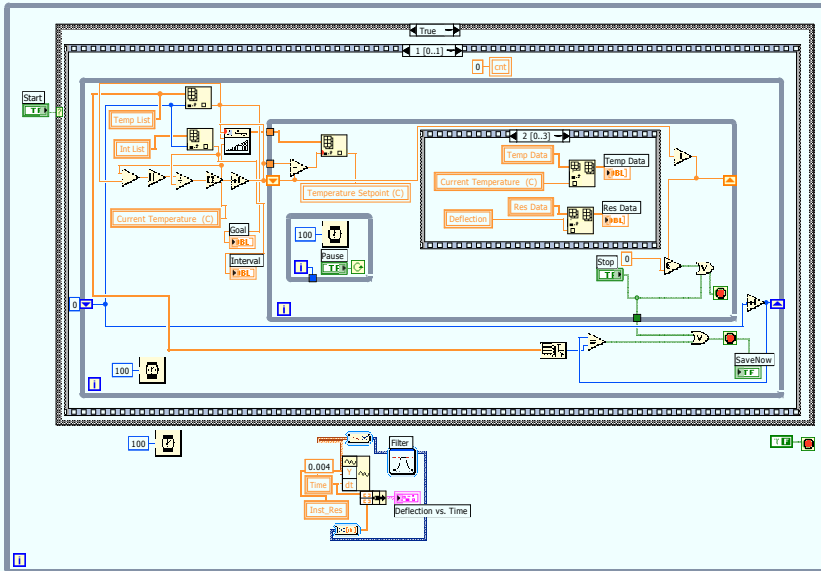
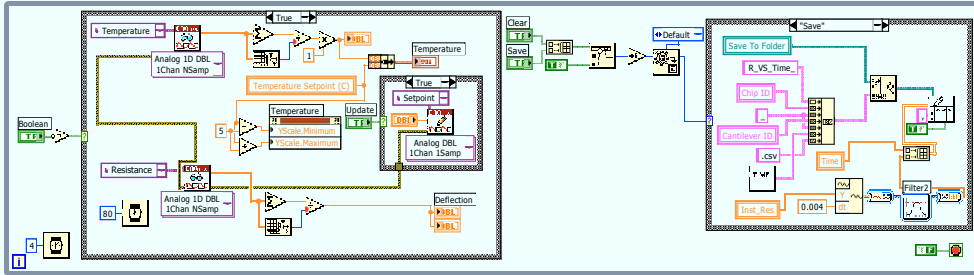


# Deflection\_vs\_Temperature.vi

C:\Documents and Settings\User\Desktop\desktop1\Deflection\_vs\_Temperature.vi

Last modified on 3/3/2011 at 9:53 PM

Printed on 4/5/2011 at 11:26 PM



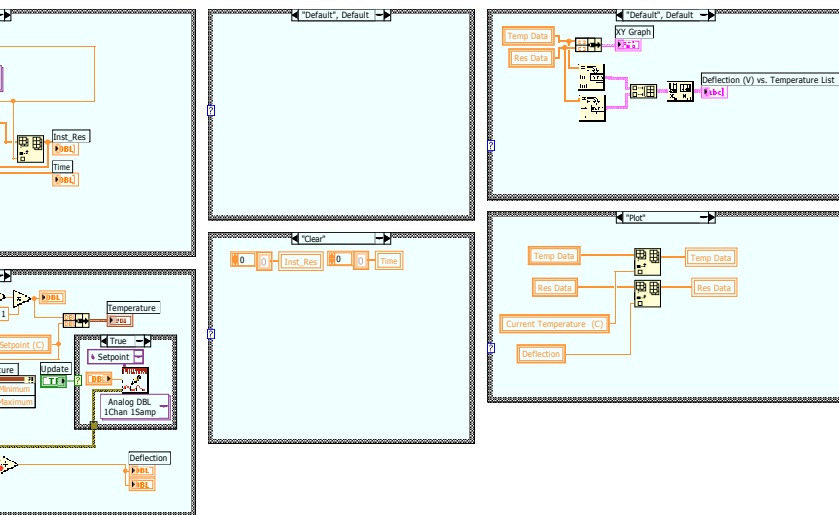


Deflection\_vs\_Temperature.vi

C:\Documents and Settings\User\Desktop\desktop1\Deflection\_vs\_Temperature.vi

Last modified on 3/3/2011 at 9:53 PM

Printed on 4/5/2011 at 11:26 PM



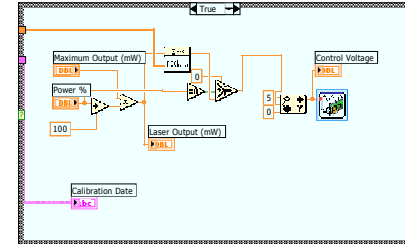
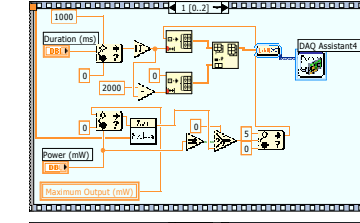
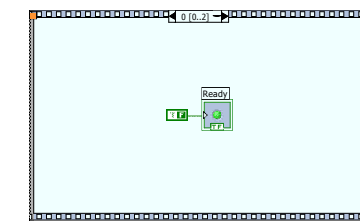
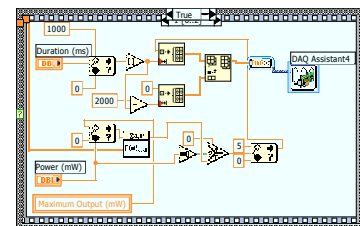
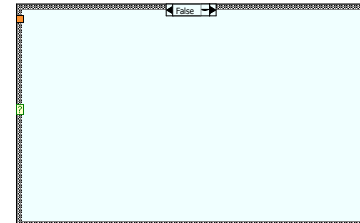
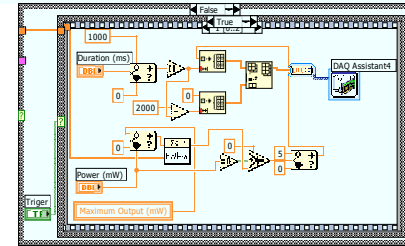
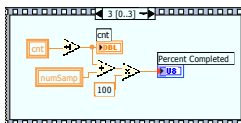
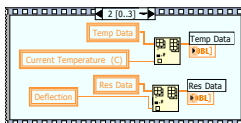
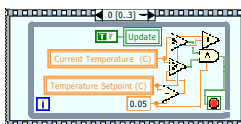
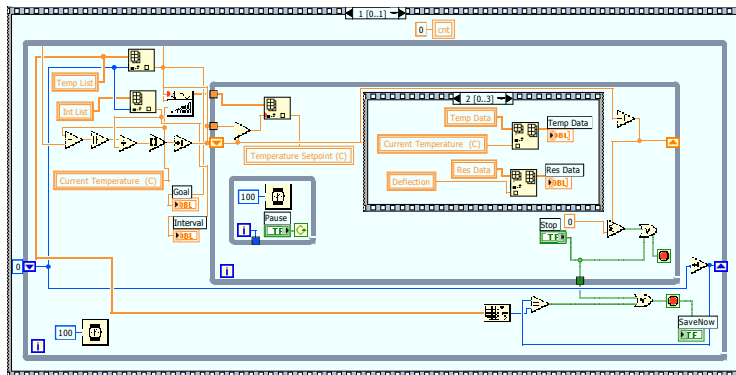
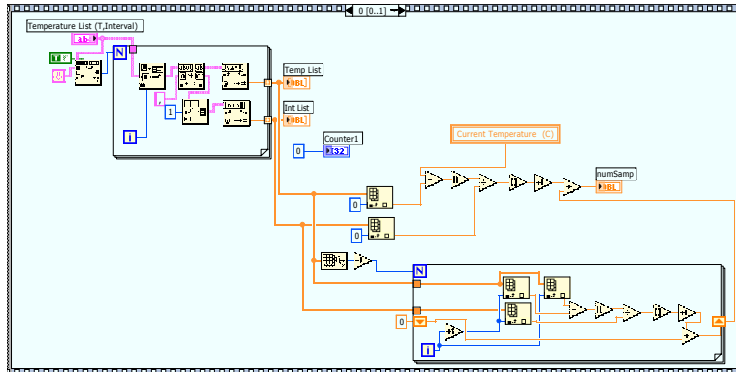
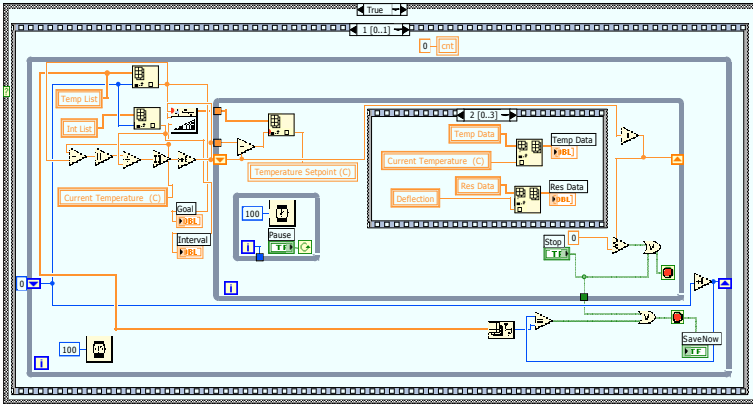


# Deflection\_vs\_Temperature.vi

C:\Documents and Settings\User\Desktop\desktop1\Deflection\_vs\_Temperature.vi

Last modified on 3/3/2011 at 9:53 PM

Printed on 4/5/2011 at 11:26 PM





# Deflection\_vs\_Temperature.vi

C:\Documents and Settings\User\Desktop\desktop1\Deflection\_vs\_Temperature.vi

Last modified on 3/3/2011 at 9:53 PM

Printed on 4/5/2011 at 11:26 PM

